Check for updates

Recovery of scandium(III) from diluted aqueous solutions by a supported ionic liquid phase (SILP)†

Dženita Avdibegović, [iD] Mercedes Regadío [iD] and Koen Binnemans [iD]*

The adsorption of scandium from diluted, acidic solutions by a supported ionic liquid phase (SILP) was investigated, as part of a process for recovery of scandium from bauxite residue (red mud). Both dry impregnation and covalent linking were studied for the SILP preparation. The SILP betainium sulfonyl(trifluoromethanesulfonylimide) poly(styrene-*co*-divinylbenzene) [Hbet–STFSI–PS–DVB] was prepared by covalent linking of the ionic liquid to the resin and this resulted in an adsorbent suitable for scandium recovery. For a chloride feed solution, the effects of pH, contact time, adsorption capacity, desorption, reusability of adsorbent and the influence of Fe(III), Al(III) and Ca(II) on the Sc(III) adsorption were studied. The adsorption of Sc(III) from nitrate and sulfate feed solution under optimal conditions was studied as well. The adsorption kinetics followed a pseudo-second order kinetic model. Equilibrium studies at room temperature showed that the experimental data could be well fitted by the Langmuir isotherm model. The stripping of Sc(III) from the loaded SILP was achieved with 1 M sulfuric acid. The SILP was stable and could be reused for seven adsorption/desorption cycles without significant losses in its adsorption efficiency for Sc(III).

Introduction

Scandium belongs to the group of rare-earth elements (REEs) and finds applications in aluminum alloys, halide lamps and fuel cells.[1] However, it is an expensive metal with small global production volumes. Although scandium is relatively abundant in the Earth's crust (22 ppm), there are few scandium minerals and it rarely occurs in rich ore deposits. It is mainly recovered as by-product from the production of other metals (REEs, U, Ti, W, Al, Ni, Ta and Nb).[2–4] Bauxite residue (red mud), the waste industrial product of the Bayer process for alumina production from bauxite ore, can contain up to 130 ppm of scandium and it is potentially a valuable scandium resource.[5,6] Scandium can partially be recovered from bauxite residue by acid leaching. Typically, in this way many metal impurities go into the leachate as well and in concentrations much higher than that of scandium.[1,7,8] Liquid–liquid extraction is used for the recovery of Sc(III),[9] but it requires much higher initial concentrations of Sc(III) than the ones that can be found in the pregnant leach solutions.[1] Nevertheless, for recovery of low concentrations of Sc(III) its enrichment with a selective adsorbent in high capacity ion exchange columns could be an efficient technique. Much of the research work on Sc(III) recovery by adsorption and extraction has been performed with resins,[10–13] modified carbon

nanotubes,[14] activated carbon,[15] SBA-15,[16] silica sol–gel material[17] or extractants impregnated onto a solid support.[18–21] Ionic liquids (ILs) show a great potential for application in hydrometallurgy, both solvent extraction[22–24] and leaching.[25,26] ILs are solvents that consist entirely of ions, and they have been investigated as non-volatile alternatives for organic solvents. However, ILs have a high viscosity which may involve drawbacks in process design. To overcome these issues different methods are used to immobilize ILs onto the surface of a solid support forming supported ionic liquid phases (SILPs).[27,28] Ideally, ILs in SILPs obtain a large specific surface area and mechanical properties of the support and maintain the extractive properties of ILs. This further makes SILPs suitable not only for applications in catalysis,[29–32] but also for metal ions adsorption and preconcentration.[28,33–35] SILPs are classified in two groups. The first group consists of the classic SILP materials where the IL is impregnated on a porous support material. The forces between the IL and the support are weak, physical Van der Waals forces (physisorption of the IL). The second group comprises covalently linked IL phases, where the IL cation (or anion) is chemically bonded to the solid support.[36] The first class of SILPs is relatively easy to prepare and these SILPs exhibit a straightforward mechanism of interactions of ILs with metal ions.[37] The main disadvantage of SILPs prepared by physisorption is the loss of the impregnated IL due to the solubility of the IL in the aqueous phase.[35,38,39] Consequently, this leads to a steady loss of adsorptive capacity and the SILPs become ineffective after several cycles of application. Moreover, leakage is not acceptable because ILs are expensive compounds and their

KU Leuven, Department of Chemistry, Celestijnenlaan 200F, P.O. Box 2404, B-3001 Leuven, Belgium. E-mail: Koen.Binnemans@kuleuven.be; Tel: +32 16 32 7446

components can contaminate the aqueous effluents.[37] In the second class of SILPs there is no discrete IL phase in the structure of the solid support. Instead, the IL can be considered as a covalently anchored ligand. Covalent linking ensures that the IL will not be leached from the support.[32,40]

The objective of this work is to develop a stable SILP for the adsorption of Sc(III) from the leach solution of industrial process residues or tailings, such as bauxite residue. To the best of our knowledge, the synthesized SILP has not been previously reported in the literature. The SILP was tested for the recovery of low concentrations of Sc(III) from acidic feed solution.

Experimental

Chemicals

AlCl$_3$·6H$_2$O (99%), nitric acid (65%), ammonia (25%), standard solutions of scandium [(1000 ± 2) µg mL^{-1}], yttrium [(1000 ± 10) µg mL^{-1}], neodymium [(1000 ± 2) µg mL^{-1}], dysprosium [(1000 ± 2) µg mL^{-1}], lanthanum [(1000 ± 10) µg mL^{-1}], gallium [(1000 ± 10) µg mL^{-1}], aluminum [(1000 ± 10) µg mL^{-1}], iron [(1000 ± 10) µg mL^{-1}] and calcium [(1000 ± 10) µg mL^{-1}] were purchased from Chem-Lab NV (Zedelgem, Belgium). Sc(NO$_3$)$_3$·5H$_2$O (99.9%), YCl$_3$·6H$_2$O (99.9%), NdCl$_3$·6H$_2$O (99.9%) were purchased from Strem Chemicals (Newburyport, USA). DyCl$_3$·6H$_2$O (99.9%) was purchased from abcr (Karlsruhe, Germany). CaCl$_2$·2H$_2$O [(100 ± 2)%] was purchased from Merck (Overijse, Belgium). FeCl$_3$ anhydrous (98%), hexadecyltrimethylammonium bromide (CTAB) (99%), betaine hydrochloride [Hbet][Cl] (99%), triethylamine (99%), and sulfuric acid (96%) were purchased from Acros Organics (Geel, Belgium). Lithium bis(trifluoromethylsulfonyl)imide (99%) was purchased from IoLiTec (Helibronn, Germany). NaOH (97%), hydrochloric acid (37%) were purchased from VWR (Leuven, Belgium). Polystyrene–divinylbenzene (PS–DVB) sulfonyl chloride resin (0.91 mmol g^{-1}, 200–400 mesh) was purchased from RappPolymere (Tübingen, Germany). Trifluoromethanesulfonamide (98%) was purchased from J&K Scientific GmbH (Pforzheim, Germany). Dichloromethane (DCM) (p.a.) and acetone (p.a.) were purchased from Fisher Chemical (Loughborough, UK). Silicone solution in isopropanol was purchased from SERVA Electrophoresis GmbH (Heidelberg, Germany). Tetraethyl orthosilicate (TEOS) (98%) and Amberlite XAD-16 resin (20–60 mesh) were purchased from Sigma Aldrich (Diegem, Belgium). Sc$_2$O$_3$ (99.99%) was cordially provided by Solvay (La Rochelle, France). Hydrated ScCl$_3$ was prepared by dissolving Sc$_2$O$_3$ in concentrated hydrochloric acid, followed by heating and evaporation of the acid near dryness. A Sc(III) stock solution (≈10 g L^{-1}) was prepared by dissolving ScCl$_3$ in ultrapure water. Working solutions of Sc(III) were prepared by diluting 10 times in ultrapure water. In order to prepare a Sc$_2$(SO$_4$)$_3$ solution, Sc(OH)$_3$ was precipitated from 5 mL of ScCl$_3$ stock solution by the addition of ammonia (25%). The precipitate was washed several times to remove the remaining chloride anions, which was confirmed by the AgCl precipitation test. The precipitate of Sc(OH)$_3$ was then dissolved in sulfuric acid and the solution was diluted with ultrapure water. The resulting solution contained ≈5 g L^{-1} of Sc(III). The concentrations of the stock solutions were measured by TXRF or ICP-OES (see next section). Amberlite XAD-16 resin

was washed prior to use according to the literature procedure and dried for 2 h in a vacuum oven at 50 °C.[41] MCM-41 silica was prepared as previously described in the literature.[42] Briefly, CTAB (2.0 g) was added to the ammonia solution, which was then homogenized. TEOS (10 mL) was added and white slurry was formed. Finally, the product was filtered, dried and calcined in the air at 550 °C for 5 h. The IL betainium bis(trifluoromethylsulfonyl)imide [Hbet][Tf$_2$N] was synthesized in a reaction between an aqueous solution of betaine hydrochloride and an aqueous solution of lithium bis(trifluoromethylsulfonyl)imide.[43]

Equipment

FT-IR spectra were recorded on a Bruker Vertex 70 spectrometer (Bruker Optics) via the attenuated total reflectance (ATR) technique with a Bruker Platinum ATR accessory. Analyses were performed with the OPUS software package. The carbon, hydrogen, and nitrogen content of the resin and SILP were determined using a CHN elemental analyzer (Thermo Scientific FLASH 2000). Scanning electron microscopy (SEM) images of platinum coated samples were recorded with Philips XL30. The specific surface area was determined by a surface area analyzer (Quantchrome NOVA 2200e). Prior to the surface area measurements, the samples were degassed under vacuum and 50 °C for 19 h. N$_2$ adsorption was measured at −196.15 °C and the Brunauer–Emmett–Teller (BET) equation was used to calculate the specific surface area. Batch adsorption and desorption experiments were performed using a VWR International water bath shaker (Type 462-0355). The synthesis of SILP was performed using Thermo Fisher Scientific MaxQ 2000 open-air platform shaker. For the desorption experiments on the recovery of Sc(III) from the loaded SILP after adsorption tests, the samples were centrifuged (Heraeus Labofuge 200). A total reflection X-ray fluorescence (TXRF) spectrometer (Bruker Picofox S2) was used to determine the concentration of Sc(III) of single-element solutions. Lanthanum internal standard was used for quantification and gallium internal standard for quality control. To avoid significant matrix effects an inductively coupled plasma-optical emission spectrometer (ICP-OES) (Perkin Elmer OPTIMA 8300) was used to determine the concentration of elements from multielement and scandium sulfate solutions. The calibration solutions and all samples were prepared by dilution with 2 wt% HNO$_3$. In order to obtain a better accuracy and precision of the ICP-OES measurement lanthanum internal standard was used. Thermogravimetric analysis (TGA) was performed on a TA Instruments T500 thermogravimeter under nitrogen flow (heating rate: 5 °C min^{-1}, from 20 up to 600 °C). The pH was measured with a Mettler-Toledo pH meter SevenCompact pH/Ion S220 after calibration with standard buffer solutions of pH 1, 4, 7 and 10.

Synthesis of SILPs

Dry impregnation method. [Hbet][Tf$_2$N] (1.0 g) was dissolved in acetone (11 mL) and Amberlite XAD-16 resin or MCM-41 silica (1.0 g) was added. The mixture was shaken for 24 h at room temperature at 300 rpm. Finally, the acetone was removed

with a rotary evaporator. The products [Hbet][Tf₂N]–Amberlite XAD-16 and [Hbet][Tf₂N]–MCM-41 silica were characterized by FT-IR (Fig. S1 and S2, ESI†). The characteristic absorption frequencies arising from the cation and anion of the IL were found in SILPs.

Covalent linking. Trifluoromethanesulfonamide (0.179 g or 1.24 mmol) was dissolved in DCM (18 mL). Polystyrene sulfonyl chloride resin (1 g, 1 eq.) and triethylamine (0.512 mL, 4 eq.) were added to the solution. The mixture was shaken for 48 h at room temperature and speed of 300 rpm on a shaking device. The resulting product (**1**) was filtered and washed with DCM. A sample of [Hbet][Cl] (0.419 g, 3 eq.) was dissolved in water (6 mL) and acetone (6 mL) was added to enhance the swelling of the resin and to make the reactive sites accessible. Then, the resulting solution of [Hbet][Cl] (**2**) was added to the intermediate product (**1**) and shaken for 24 h at room temperature at 300 rpm. The final product (**3**) was filtered, washed with acetone and finally with ultrapure water. The obtained wet product was used in the batch adsorption experiments. The SILP and the sulfonyl chloride resin were dried at 50 °C for 24 h in a vacuum oven prior to FT-IR, SEM, CHN analysis and TGA for determining the decomposition temperature. FT-IR was used to characterize the SILP (Fig. S3 and Table S1, ESI†). The most characteristic peaks in the IR spectra of the SILP were the C=O asymmetric stretching in the carboxylic group of the cation at 1750 cm⁻¹ and S=O asymmetric stretching which shifted from 1375 cm⁻¹ in the SILP, indicating that the reaction between sulfonyl chloride group and trifluoromethanesulfonamide has taken place.[44,45]

Adsorption and desorption tests

For batch adsorption experiments 0.05 g of wet SILP prepared by the covalent linking was added to 10 mL of an aqueous solution of Sc(III) in a 20 mL glass vial. Unless otherwise specified, the concentration of Sc(III) was 1.1 mmol L⁻¹, the shaking speed 300 rpm and the equilibration time 90 min. The experiments were carried out at room temperature in chloride media. The pH was adjusted between 0.5 and 3.5 using diluted HCl (or other corresponding acid: H₂SO₄ in sulfate and HNO₃ in nitrate media) or NaOH solution. After equilibration the solutions were filtered through a cellulose syringe filter with a pore size of 0.45 μm. The pH of the filtrate was measured and the metal ion concentration was determined by TXRF or ICP-OES. The amount of the metal ions adsorbed onto the SILP was calculated from the eqn (1):

$$q = \frac{(c_{in} - c_{eq})V}{m_{ads}} \tag{1}$$

where q is the amount of adsorbed metal ions at equilibrium (mmol g⁻¹ of dry adsorbent), c_{in} is the initial metal ion concentration in the solution (mmol L⁻¹), c_{eq} is the equilibrium concentration of metal ions in the solution (mmol L⁻¹), V is the volume of the solution (L) and m_{ads} is the mass of the dry adsorbent (g), calculated based on the moisture in the SILP obtained from the TGA data (Fig. S4, ESI†). The estimated average moisture content was 32%. Desorption and recovery of metal ions from the loaded SILP was performed with 2 mL of the tested acids (HCl, HNO₃ and H₂SO₄). Prior to the addition of

acid, the solution was centrifuged for 2 min at 3000 rpm and the supernatant was taken by a pipette. The SILP was washed two times with 10 mL of ultrapure water to remove eventually residual metal ions and centrifuged again. The same procedure was applied for the reusability studies under the optimized conditions, where after each desorption and washing step 10 mL of Sc(III) feed solution was added. The desorbed amount (%) was calculated from eqn (2):

$$\text{Desorption } (\%) = \frac{c_2}{c_1} \times 100 \tag{2}$$

where c_2 is the concentration of metal ions in the solution after desorption at equilibrium and c_1 (mmol L⁻¹) is represented by eqn (3):

$$c_1 = \frac{(c_{in} - c_{eq})V}{V_{ac}} \tag{3}$$

where V_{ac} (L) is the volume of acid used for desorption.

Stability tests of SILPs prepared by the dry impregnation method

TGA was used to estimate the amount of IL prior to and after performing the Sc(III) adsorption tests with SILPs prepared by a dry impregnation method. A 0.10 g of impregnated SILPs was added to 5 mL of aqueous solutions containing 2.2 mmol·L⁻¹ of Sc(III). The experiments were carried out at room temperature, a shaking speed of 300 rpm and an equilibration time of 90 min. The initial pH was adjusted to 3.5. After equilibrating, the mixtures were centrifuged for 2 min at 3000 rpm. The supernatant was taken by a pipette for TXRF analysis of the Sc(III) concentration. The remaining SILPs were dried in a vacuum oven for 24 h at 50 °C prior to the TGA measurements. The content of the IL in SILPs was estimated from the observed percentage of mass loss in the temperature range of the IL decomposition.

Results and discussion

SILPs characterization

The dry impregnation method was employed for the preparation of SILPs containing the ionic liquid [Hbet][Tf₂N], which is known to be a good extractant for Sc(III) (Fig. 1).[7] Two solid supports were tested for impregnation of [Hbet][Tf₂N] : Amberlite XAD-16 and MCM-41 silica. Amberlite XAD-16 resin exhibits a high surface area (≈800 m² g⁻¹) and large pore volumes (200 Å).[40] The support with a polystyrene–divinylbenzene (PS–DVB) matrix is unlikely to affect the metal ion adsorption processes. Therefore, only the IL will play an active role in the adsorption process.
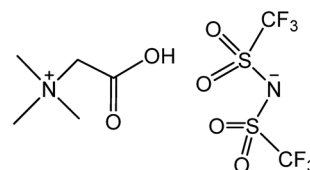

Fig. 1 Chemical structure of the IL [Hbet][Tf₂N].

MCM-41 silica was selected as a support because it is one of the most important members of the family of mesoporous molecular sieves.[46] Mesoporous silicas are often used as solid supports due to their large surface area (≈ 1000 m^2 g^{-1}), fast adsorption kinetics and controllable pore size (between 2 and 50 nm) and pore arrangement.[47] It was not possible to precisely determine the IL content in the Amberlite XAD-16 SILP by TGA, because of the overlapping of thermal decomposition of the IL and Amberlite XAD-16 between 300 and 500 °C (Fig. 2a). However, the change in the height drop of the TGA curve of the tested SILP in the temperature range from 300 to 400 °C indicated that the content of the IL after one adsorption test had decreased from 50 wt% to approximately 20 wt%. From the TGA data (Fig. 2b) the estimated amount of the IL in the SILPs after impregnation of the MCM-41 silica was ≈ 50 wt%. There was a clear distinction between the decomposition temperature of the IL and the MCM-41 silica support. The content of the IL in the silica-based SILP after one batch adsorption test had decreased from 50 wt% to approximately 13 wt%. In addition to the losses of IL from both supports, the reproducibility of the Sc(III) adsorption results was poor due to the solubility of the IL in the acidic aqueous feed

solution. According to previous studies, the solubility of [Hbet][Tf$_2$N] in water (1 : 1 ratio) is approximately 14 wt%, if no high concentrations of salting-out agents are present.[7] When testing the stability and adsorption properties of SILPs with impregnated [Hbet][Tf$_2$N] high liquid-to-solid ratios were applied (50 : 1). Therefore a higher solubility of the IL was anticipated than in the case of liquid–liquid extraction. Even with supports exhibiting a high surface area, the IL loading of 50 wt% could not be maintained over time and severe IL losses occurred. The solubility of [Hbet][Tf$_2$N] can potentially be decreased by addition of salting-out agents to the aqueous phase (for instance Na$_2$SO$_4$) to further optimize the adsorption procedure.[26] However, this was not applied in this study because it would require high inorganic salts consumption. Additionally, the ions of the inorganic salt may interfere in the downstream processes to recover pure scandium in a high yield.

Because of the losses of IL from the SILPs prepared by impregnation, covalent linking of the IL onto the support was performed. Carboxylic acid extractants and ILs with a carboxyl functional group are useful for extraction and separation of metal ions.[9–11,48–50] In this study a SILP mimicking the structure of [Hbet][Tf$_2$N] was synthesized (Fig. 3). El Kadib *et al.* previously reported the synthesis of a SILP prepared by covalent linking with periodic mesoporous organosilica and trisilylated guanidinium-sulfonimide IL.[51] The IL was covalently anchored to the silica surface *via* both the organo-cationic and the organo-anionic moieties.[51] Instead of preparing the silylated sulfonamide precursor for surface grafting to SBA-15 and MCM-41 silica, the SILP was synthesized starting from a PS–DVB-based resin as a support with sulfonyl-chloride reactive sites. Silica-based materials suffer from a lack of stability in strongly acidic or alkaline conditions, low breakthrough for polar analytes,[40] collapse of the mesoporous structure in water due to silicate hydrolysis[47] and the need to use more expensive starting compounds such as 2-(4-chlorosulfonylphenyl)ethyl-trimethoxysilane instead of a sulfonyl chloride resin.

Polymer-based supports have better tolerance towards samples and eluents with extreme pH values and moreover PS–DVB resins show high mechanical rigidity and stability,[52] making them convenient for preparing adsorbents that are used in highly acidic media. A sulfonimide was thus synthesized by reaction of PS–DVB sulfonyl chloride resin and tri-fluoromethanesulfonamide in the presence of excess of triethylamine (top Fig. 3). By the addition of excess amount of betaine hydrochloride the triethylammonium cation was then exchanged for betainium (bottom Fig. 3). In the final synthesis step, acetone was used to enhance the swelling of the support. If
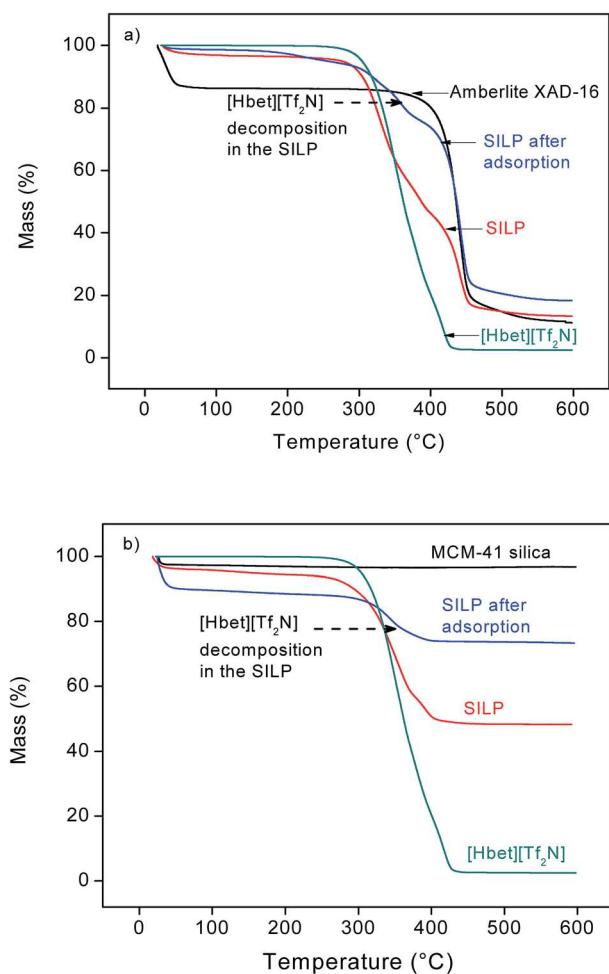

Fig. 2 TGA of the SILPs [Hbet][Tf$_2$N]–Amberlite XAD-16 (a) and [Hbet][Tf$_2$N]–MCM-41 silica (b) prior and after the adsorption test. Nitrogen atmosphere, heating rate: 5 °C min^{-1}, from 20 to 600 °C.
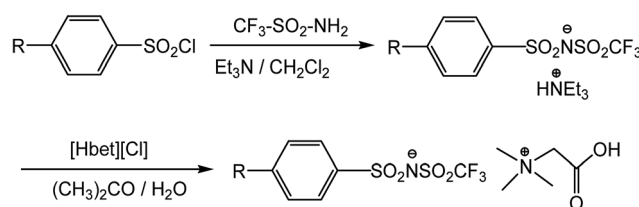

Fig. 3 Synthesis of the SILP Hbet–STFSI–PS–DVB.

the support is not well swollen, the accessibility of the reactive sites is poorer and the reaction rates are slower. Therefore, the reaction solvent must be carefully chosen since cross-linked polystyrene resins will not swell in solvents that are too polar like water.[42,43,53] If the resin is sufficiently porous, the reactive sites are accessible even without extensive swelling. Still, it is necessary that the resin swells to accommodate larger organic ions during the synthesis of the SILP.[54]

Moreover, the CHN analysis results for sulfonyl chloride resin were: 81.12% C, 7.12% H and 0.00% N. The synthesis of the SILP by covalent linking was confirmed by the presence of nitrogen in the SILP: 71.64% C, 6.30% H and 1.81% N. From the N content the degree of functionalization of the sulfonyl chloride resin was estimated to be around 71%. The BET specific surface area of the resin was 49 $m^2 g^{-1}$, while when accommodating the ion pairs in the SILP the specific surface area decreased to 15 $m^2 g^{-1}$. The SILP had the same spherical shape as the resin that was used as support (Fig. 4).

Sulfonyl chloride resin with particle size between 200 and 400 mesh was selected as a starting material for the synthesis. Adsorbents with too small particle size can cause issues with phase separation in batch adsorption experiments. Furthermore, if applied in column chromatography separations, issues with leakage or clogging might occur. On the other hand, if the particle size is large, it can negatively affect the adsorption kinetics and the adsorption capacity, since the uptake by smaller particles is more favoured due to greater accessibility of the functional groups.[55]
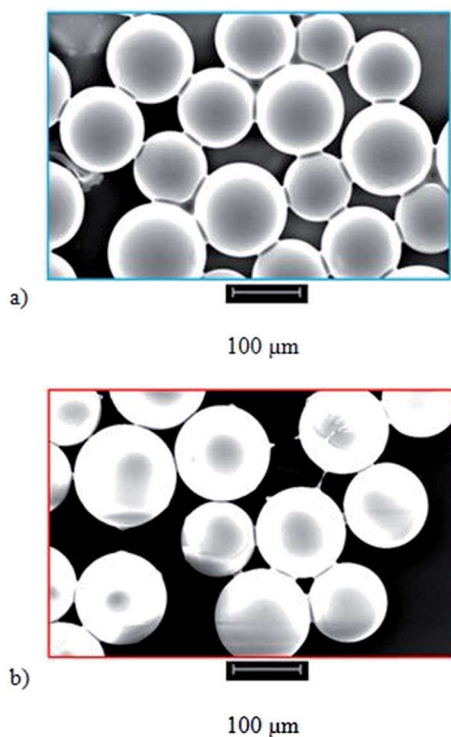

Fig. 4 SEM images of sulfonyl chloride resin (a) and SILP Hbet−STFSI−PS−DVB (b). Acceleration voltage 10.0 kV, working distance 10.0 mm, 500× magnification.
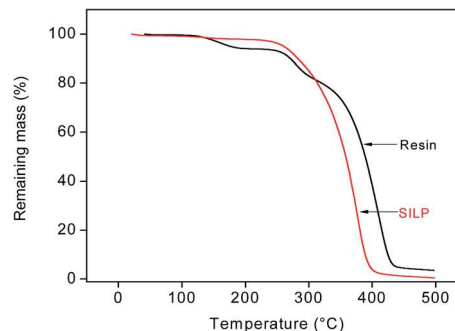

Fig. 5 TGA of sulfonyl chloride resin and the SILP Hbet−STFSI−PS−DVB. Nitrogen atmosphere, heating rate: 5 °C min^{-1}, from 20 to 500 °C.

To examine whether the thermal stability of the SILP differed significantly from the starting resin, a TGA of both materials was performed. In the sulfonyl chloride resin, the thermal decomposition of polystyrene matrix was between 320 and 440 °C (Fig. 5). The thermal decomposition of the SILP started at a lower temperature, but above 200 °C. With the covalent attachment of ion pairs onto the resin, the thermal stability range of the polymer support was slightly decreased (>95% of the polystyrene was decomposed at 410 °C). In general, the working temperatures for metal adsorption from aqueous solution are below 100 °C. Thus, the slight decrease in the thermal stability range of the polymer support after covalent linking of ion pairs does not diminish the usability of the SILP in metal ion separation.

Effect of pH

To recover Sc(III) from acidic leachates, a convenient adsorbent must have the property of adsorbing Sc(III) at low pH. To prevent the precipitation of Sc(OH)$_3$, the pH was kept below 4 (although the actual pH at which Sc(OH)$_3$ starts to precipitate depends on the scandium concentration).[7,56] The same consideration has to be taken into account for the common accompanying elements in the bauxite residue leachates which are present in significantly higher concentrations than Sc(III). Losses of Sc(III) by coprecipitation of other metal hydroxides might occur. For instance, in bauxite residue leach solutions the concentration of Sc(III) is only a few ppm compared to the thousands of ppm for major elements (Fe, Al, Ca, Si, Ti).[1] Therefore, the effect of the initial pH on Sc(III) adsorption was investigated for the range 0.5 < pH < 3.0 and the equilibrium pH was monitored as well (Fig. 6). With the increase in initial pH, the adsorption of Sc(III) also increased, accompanied by a decrease in equilibrium pH. Even at pH < 1.5, the amount of adsorbed Sc(III) is in the same range as observed for adsorbents that have been previously used for Sc(III) recovery from bauxite residue leach solutions.[57] Furthermore, over the entire investigated acidic pH range the SILP showed superior adsorption capacity for Sc(III) over previously reported adsorbents selective for scandium.[16,58] Therefore the SILP could be considered as a suitable adsorbent for recovery of Sc(III) from acidic media.

Furthermore, the adsorption mechanism under acidic conditions and the stability of the SILP under basic conditions
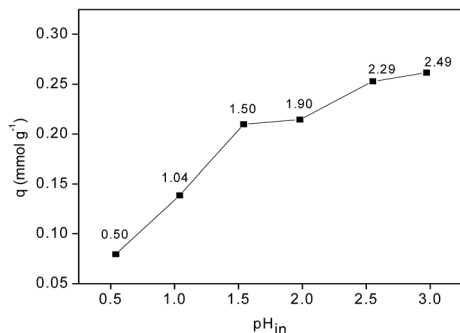
Fig. 6 Effect of the initial (pH$_{in}$) and equilibrium pH (pH$_{eq}$ values are labeled in the graph) on Sc(III) adsorption with SILP Hbet−STFSI−PS−DVB: aqueous phase = 10 mL, 0.05 g of SILP, Sc(III) concentration 1.1 mmol L^{-1}, 90 min, 300 rpm, room temperature.

was investigated by FT-IR (Fig. 7). The stability of the SILP in basic solution was studied to compare its behavior with the IL [Hbet][Tf$_2$N]. [Hbet][Tf$_2$N] alkali-metal salts are water soluble and in alkaline solutions the IL becomes completely water miscible.[53] A sample of 0.05 g of wet SILP was added to 1 mL of 5.1 mmol L^{-1} Sc(III) (pH$_{in}$ = 2.8, pH$_{eq}$ = 2.5) and NaOH solution (pH$_{in}$ = 12.9). The samples were shaken for 3 h at 1000 rpm and afterwards centrifuged. The remaining SILP was washed with ultrapure water and dried for 24 h in a vacuum oven at 50 °C. The absorption band at 1750 cm^{-1} that corresponds to the COOH group had shifted to 1649 cm^{-1} after Sc(III) adsorption and to 1664 cm^{-1} after Na(I) adsorption. The later absorption bands correspond to the conjugated base COO$^-$, which confirmed that the presence of the betainium cation in the SILP Hbet−STFSI−PS−DVB is essential for adsorption of Sc(III). Moreover, a similar SILP with the Et$_3$N$^+$ cation instead of the betainium cation (top Fig. 3) was not able to adsorb Sc(III) from aqueous solution, due to the lack of carboxylic functional group. These findings are similar to what was observed for liquid–liquid extraction of Sc(III) when using the ionic liquids [Hbet][Tf$_2$N][7] and tri-n-butyl(carboxymethyl)-phosphonium chloride, [P$_{444}$C$_1$COOH][Cl].[48] Unlike the IL [Hbet][Tf$_2$N], when mixed with a NaOH solution (pH = 12.9) the SILP Hbet-STFSI−PS−DVB

did not lose its ion pairs to the aqueous phase. This was evident from the presence of the COO$^-$ absorption band. In principle, the miscibility of ILs depends on its ionic species. In the SILP, the IL was covalently attached via the anion to the polymer which strongly contributed to the stability of the SILP even in alkaline solutions.

Sc(III) adsorption isotherms from different media

The adsorption of Sc(III) at room temperature was studied from chloride, nitrate and sulfate media since the corresponding acids can be used for leaching of metals from bauxite residue. Scandium(III) chloride, nitrate and sulfate salts were used to prepare the tested feed solution. On the one hand, from chloride and nitrate media, Sc(III) adsorption with the SILP Hbet−STFSI−PS−DVB increased with the increase in initial and equilibrium Sc(III) concentration. In principle, rare-earth chloride and nitrate negatively charged complexes are not stable at low chloride and nitrate concentrations, and REEs are present as hydrated metal ions.[59] On the other hand, the adsorption in sulfate media was low (Fig. 8). This can be explained by the formation of scandium(III) sulfate complexes. Schrodle et al. showed that Sc(III) in sulfate media forms both inner- and outer-sphere 1 : 1 [ScSO$_4$]$_{(aq)}$$^+$ complexes.[60] Higher-order inner-sphere complexes predominate in more concentrated solutions of scandium sulfate, and most likely fac-[Sc(SO$_4$)$_3$(OH$_2$)$_3$]$^{3-}$ is the major species present. The electrostatic interactions of small Sc(III) ions (0.745 Å for coordination number of 6)[2] with the sulfate ligands are strong, which makes the adsorption of Sc(III) by the SILP via H$^+$ exchange difficult.

The Langmuir and Freundlich adsorption models were applied to describe the sorption process of Sc(III) from chloride and nitrate media.[61] Although these models do not provide information about the type of reaction involved, the effect of ionic strength, the pH or the composition of the media, they are widely used as empirical models to describe very simply the adsorption. Thus, they can provide an estimate for the maximum adsorption capacity and the type of adsorption.[62]

The linearized Langmuir equation is given by eqn (4):

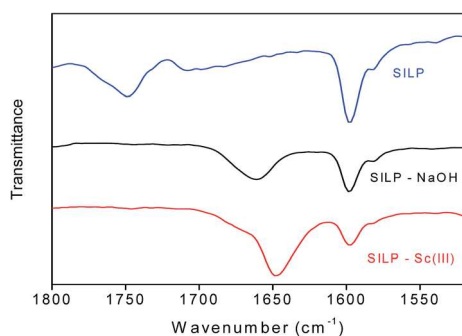$$\frac{c_{eq}}{q} = \frac{1}{K_L q_m} + \frac{c_{eq}}{q_m} \tag{4}$$

Fig. 7 FT-IR spectra of the carboxylic acid/carboxylate peak of the SILP Hbet−STFSI−PS−DVB before adsorption tests and adsorption under acidic and alkaline conditions: aqueous phase = 1 mL, 0.05 g of SILP, 270 min, 1000 rpm, room temperature. pH of NaOH solution = 12.9. Sc(III) concentration = 5.1 mmol L^{-1}, pH$_{in}$ = 2.8, pH$_{eq}$ = 2.5.
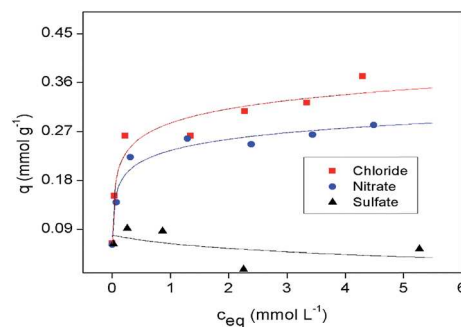

Fig. 8 Sc(III) adsorption from chloride, nitrate and sulfate media with the SILP Hbet−STFSI−PS−DVB. The initial Sc(III) concentration was varied between 0.2 and 5.6 mmol L^{-1}, pH$_{in}$ = 3.0, 90 min, 300 rpm, room temperature.

where c_{eq} is the concentration of Sc(III) at equilibrium (mmol L^{-1}), q is the amount of Sc(III) adsorbed by dry SILP (mmol g^{-1}), K_L is the Langmuir constant (L mmol^{-1}), q_m is the maximum adsorption capacity (mmol g^{-1}).

The linearized Freundlich equation is represented by eqn (5):

$$\log q = \log K_F + \frac{1}{n}\log c_{eq} \qquad (5)$$

where K_F is Freundlich isotherm constant and n is the adsorption intensity. A plot of $\log q$ *versus* $\log c_{eq}$ represents the Freundlich adsorption isotherm at room temperature. Adsorption of Sc(III) in chloride and nitrate media follows the Langmuir adsorption isotherm model with correlation coefficient of 0.98 and 0.99, respectively (Table 1, Fig. S5 and S6, ESI†). Freundlich adsorption isotherms gave correlation coefficients of 0.87 in chloride and 0.91 in nitrate media. According to the Langmuir model, the total concentration of the adsorbed compound increases when its concentration in the aqueous solution increases. This model suggests that adsorption occurs on a homogenous monolayer surface where the number of sorption sites is finite and once a sorbate molecule occupies a site, no further sorption can take place at that site.[55,62]

Kinetic study

In order to examine the controlling step for adsorption mechanism, the widely used pseudo-first-order and pseudo-second-order models were applied. The Lagergren linearized pseudo-first-order kinetic model is given by the eqn (6):[61,63,64]

$$\log(q_m - q_t) = \log q - \frac{k_1}{2.303} \times t \qquad (6)$$

where q_m and q_t are the amounts (mmol g^{-1}) of metal ions per amount of dry adsorbent (g) at equilibrium and at time t, respectively; k_1 is the pseudo-first-order rate constant (min^{-1}).

The linear form of pseudo-second-order kinetic model given by Ho and McKay can be represented by the eqn (7):[61,64,65]

$$\frac{t}{q_t} = \frac{1}{k_2 q^2} + \frac{t}{q_m} \qquad (7)$$

where q_m and q_t are the amounts (mmol g^{-1}) of Sc(III) ions per amount of dry adsorbent (g) at equilibrium and time t (min), respectively; k_2 is the pseudo-second-order rate constant (g mmol^{-1} min^{-1}). The Sc(III) adsorption kinetics data fitted well to the pseudo-second-order kinetics model (Fig. S7, ESI†)

(correlation coefficient of 0.99, from the plot of tq_t^{-1} against t) contrary to a low correlation coefficient when applying the pseudo-first-order kinetics model (0.53). This suggests that the reaction rate is controlled by a chemisorption process. It involves formation of chemical bonds through sharing or exchanging of electrons between adsorbent and adsorbate.[64] The SILP exhibited fast kinetics and within 15 min equilibrium was reached (Fig. 9). This is a significant improvement in adsorption kinetics in comparison with some conventional resins (6 to 48 h).[66,67] The values of q_m and k_2 were calculated from the slope and intercept of the straight line (Fig. S7, ESI†) and are equal to 0.30 mmol g^{-1} and 2.78 g mmol^{-1} min^{-1}, respectively. In the batch adsorption experiments, a wet SILP was used (average water content of 32 wt%) since drying can cause increase in the hydrophobicity and collapse of the structure rendering reactive sites inaccessible and thereby affecting adsorption kinetics.[39,68,69] Moreover, when using adsorbent in column chromatography, the adsorbent is in general preconditioned before it is added to the column, and therefore the wet adsorbent would even better reflect the behaviour of the SILP in column chromatography separations.[70]

Effect of interfering ions

The adsorption of Sc(III) in the presence of other associated major elements in secondary resources (*e.g.* bauxite residue) such as Fe(III), Al(III) and Ca(II) was investigated.[1] Multi-element, equimolar solutions were investigated in order to elucidate the adsorption preference of the selected ions. The selectivity was tested under acidic conditions (pH from 0.5 to 1.8), to assure that no hydrolysis would occur, especially of Fe(III). The same trend of increase in adsorption efficiency with the increase of pH was observed as with single element solutions. Moreover Sc(III) was preferentially adsorbed over the other tested elements (Fig. 10). Two main factors could have contributed to the selectivity of the SILP: the electrostatic interactions and the hydration energy. A general rule is that ion-exchangers adsorb ions following the order starting from the higher valence, because the electrostatic attraction is directly proportional to the ionic charge and inversely proportional to the ionic radius.[71]
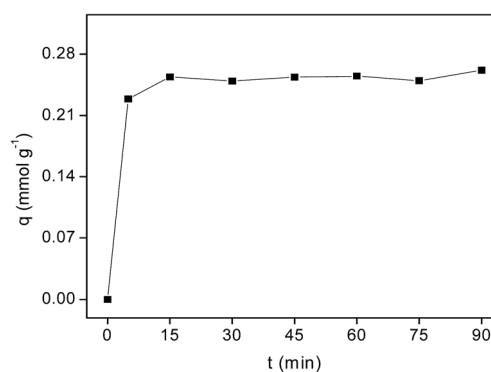
Table 1 Adsorption isotherm data for Sc(III) adsorption from chloride and nitrate media at room temperature

Isotherm model	Parameter	Chloride media	Nitrate media
Langmuir	q_m (mmol g^{-1})	0.36	0.29
	K_L (L mmol^{-1})	5.68	10.0
	R^2	0.98	0.99
Freundlich	K_F (mmol^{1-n} g^{-1} L^n)	0.11	0.10
	n	4.18	4.62
	R^2	0.87	0.91

Fig. 9 Kinetic study of Sc(III) adsorption with SILP Hbet−STFSI−PS−DVB: aqueous phase = 10 mL, 0.05 g of SILP, Sc(III) concentration 1.1 mmol L^{-1}, pH$_{in}$ = 3.0, pH$_{eq}$ = 2.5, 300 rpm, room temperature.
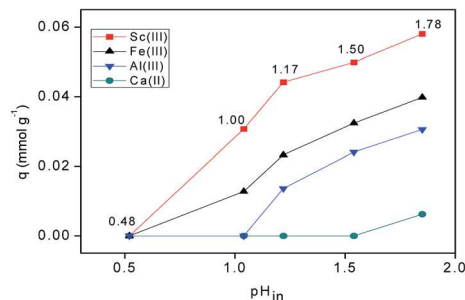
Fig. 10 Influence of initial (pH_{in}) and equilibrium pH (pH_{eq} values are labeled in the graph) on the adsorption of major elements and Sc(III) with the SILP Hbet–STFSI–PS–DVB: aqueous phase = 10 mL, 0.05 g of SILP, multi-element equimolar solution with total concentration of elements 1.1 mmol L^{-1}, 90 min, 300 rpm, room temperature.

Fig. 12 Influence of initial (pH_{in}) and equilibrium pH (pH_{eq} values are labeled in the graph) on the adsorption of REEs with the SILP Hbet–STFSI–PS–DVB: aqueous phase = 10 mL, 0.05 g of SILP, multi-element equimolar solution with total concentration of elements 1.1 mmol L^{-1}, 90 min, 300 rpm, room temperature.
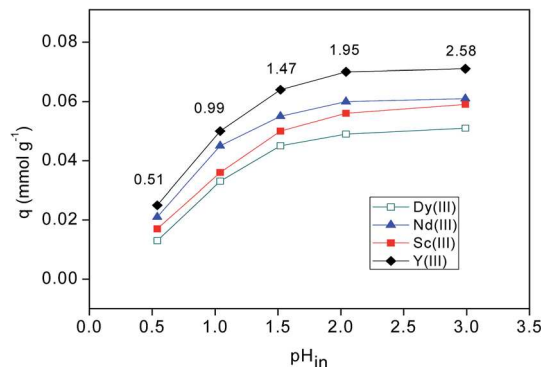
Therefore Ca(II) ions were least adsorbed by the SILP. Another factor is hydration energy. Among trivalent ions hydration enthalpies follow the trend Sc > Fe > Al, which is in an agreement with the selectivity of the SILP.[72] According to Eisenman's model for selectivity of adsorbents the less hydrated ions are easier to dehydrate and, therefore, these are more likely to be selectively adsorbed by the exchanger.[73] In conclusion, valence and hydration energy could explain the preferential uptake of ions by the SILP. Since Sc(III) and Fe(III) have similar chemical behaviour and the expected concentration of Fe(III) in leach solutions is significantly higher than that of Sc(III), the selectivity of the SILP was further tested from a binary solutions of Sc(III) and Fe(III) at pH ≈ 1.0 (Fig. 11). From the binary equimolar solution Sc(III) was preferentially adsorbed. With the increase of Fe(III) concentration, the amount of adsorbed Sc(III) decreased. When the initial concentration of Fe(III) was five times higher than that of Sc(III), the amount of adsorbed Sc(III) decreased up to 47% of the amount adsorbed from the binary equimolar solution. These results suggest that Fe(III) should be removed as much as possible (for instance by smelting reduction)[74] prior to the preconcentration of Sc(III) with the SILP. Previously reported adsorbents incorporating carboxylic group were found to be suitable for selective Sc(III) adsorption over major elements [chitosan–silica adsorbent functionalized with ethyleneglycol tetraacetic acid (EGTA), resin with glycol amic
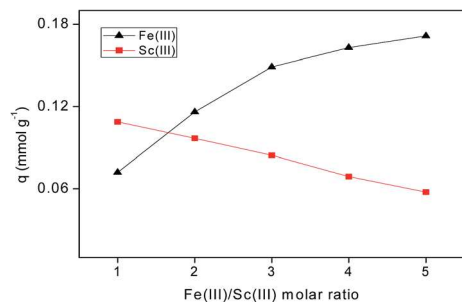
acid group].[10,57] In terms of selectivity over major elements compared with reported adsorbents the SILP showed lower performance in batch adsorption experiments. However, accounting other important parameters like kinetics, adsorption capacity under acidic conditions, preferential uptake of Sc(III) over major elements from equimolar solutions and relatively simple synthesis procedure, would justify the use of the SILP for further optimization for Sc(III) recovery.

Moreover, the SILP was tested for the adsorption of Sc(III) in the presence of other REEs that can be found in bauxite residue [Y(III), Nd(III) Dy(III)].[1] Over the investigated pH range (from 0.5 to 3.0) from multielement solutions all REEs were adsorbed by the SILP (Fig. 12). Selectivity of the SILP for Sc(III) over other REEs was therefore not superior to previously reported metal phosphate ion-exchangers applied for Sc(III) recovery from bauxite residue.[75,76] However, results imply that the SILP could be used for adsorption of REEs from acidic media and then Sc(III) could be further separated from other elements in a chromatography column (after optimizing chromatographic conditions such as proper eluent, flow rate *etc.*).

Desorption and reusability of the SILP Hbet–STFSI–PS–DVB

In order to recover Sc(III) from the SILP the desorption efficiency of HCl, HNO_3 and H_2SO_4 was investigated. The desorption efficiency increased with an increase in acid concentration (Fig. 13). Quantitative (100%) desorption of Sc(III) was possible even with 1 mol L^{-1} H_2SO_4. Eluting with 2 mL of H_2SO_4 resulted in a fourfold Sc(III) concentration compared to its initial concentration. This indicates that the covalent SILP Hbet–STFSI–PS–DVB could be used for preconcentration of Sc(III) from diluted solutions using chromatography, provided that the concentration of major interfering ions is minimized, especially of Fe(III). The fact that the highest desorption efficiency corresponds to H_2SO_4 could be attributed to scandium sulfate complex formation, as previously discussed.

To apply the synthesized SILP Hbet–STFSI–PS–DVB for the recovery of Sc(III) in a scaled-up process, the SILP has to be reusable. Thus, the SILP was tested in a seven consecutive

Fig. 11 Fe(III)/Sc(III) selectivity for the SILP Hbet–STFSI–PS–DVB: aqueous phase = 10 mL, 0.05 g of SILP, c_{in}[Sc(III)] = 1.1 mmol L^{-1}, c_{in}[Fe(III)] from 1.1 mmol L^{-1} to 5.5 mmol L^{-1}, $pH_{in} ≈ pH_{eq} ≈ 1.0$, 90 min, 300 rpm, room temperature.
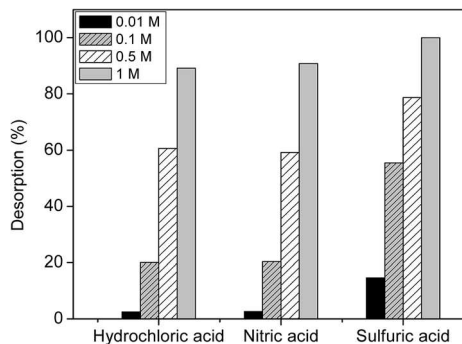
Fig. 13 Desorption (%) of Sc(III) with different concentration of acids (2 mL of HCl, HNO$_3$, H$_2$SO$_4$) from 0.05 g of SILP Hbet–STFSI–PS–DVB previously loaded with $\approx$ 0.2 mmol g^{-1} of Sc(III). Desorption conditions: 30 min, 300 rpm, room temperature.
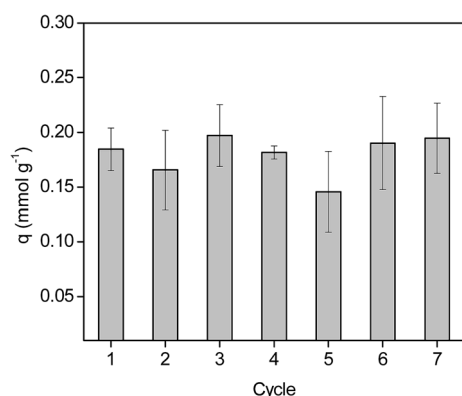

Fig. 14 Reusability of SILP Hbet–STFSI–PS–DVB by desorption with 2 mL of 1 mol L^{-1} H$_2$SO$_4$, previously loaded with $\approx$ 0.2 mmol g^{-1} of Sc(III). Adsorption/desorption time 30 min, 300 rpm, room temperature.

adsorption/desorption cycles, in duplicate. The complete desorption of the previously adsorbed Sc(III) was performed with 1 mol L^{-1} H$_2$SO$_4$ (Fig. 13). From one cycle to the next one, there were random differences in the adsorption of Sc(III) (Fig. 14). These variations can more likely be attributed to the experimental errors of the batch tests. The adsorbed amount of Sc(III) in the first cycle was comparable to the amount adsorbed in the last two cycles. The insignificant difference between the q value of each cycle and the mean q value was additionally confirmed by Wilcoxon's statistical test (Table S2, ESI†). Thus, it can be concluded that adsorption efficiency of the SILP did not significantly change. In batch adsorption studies of the reusability of a SILP, the source of random errors arises from the potential losses of adsorbent during handling or dilution of the fresh feed by the residual amount of ultrapure water used for pretreatment between the cycles. However, the reproducibility of the results was achieved probably due to the covalent bonding of the IL onto the support. This additionally confirmed the success in the preparation of a sustainable adsorbent material for Sc(III) recovery from acidic aqueous solutions.

Conclusion

The SILP-based adsorbent for Sc(III) recovery, which was synthesized by covalent linking of ion pairs, showed good adsorption properties for Sc(III) from acidic aqueous solutions. The formation of Sc(III) sulfate complexes resulted in a low adsorption efficiency, but high desorption efficiencies. From chloride and nitrate media the adsorption was effective and followed a Langmuir adsorption isotherm. The pseudo-second-order kinetic model best describes the kinetic adsorption processes of Sc(III) by the SILP. In addition, when using the SILP Hbet–STFSI–PS–DVB short contact time were sufficient (15 min) due to the fast adsorption kinetics. In the presence of other common impurities such as Fe(III), Al(III) and Ca(II), the highest adsorption efficiency of the SILP was found for Sc(III) when equimolar solutions were used. However, in the presence of substantially higher concentrations of Fe(III), the Sc(III) adsorption decreased. In batch experiments, the quantitative desorption for the recovery of the Sc(III) adsorbed on the SILP with H$_2$SO$_4$ was shown and reusability of the SILP without affecting its efficiency after repeating the process seven times. Moreover, the loss of the IL to the aqueous phase was prevented. Thus, SILPs can be designed as adsorbents for the recovery and separation of targeted elements. The complete separation of Sc(III) from other accompanying elements can be optimized, for instance, in chromatography columns and further work in this field is undergoing in our laboratory.

Conflicts of interest

There are no conflicts to declare.

Acknowledgements

References

1 C. R. Borra, Y. Pontikes, K. Binnemans and T. Van Gerven, *Miner. Eng.*, 2015, **76**, 20–27.

2 S. A. Cotton, *Polyhedron*, 1999, **18**, 1691–1715.

3 W. Wang, Y. Pranolo and C. Y. Cheng, *Hydrometallurgy*, 2011, **108**, 100–108.

4 EMC Metals Corporation (TSX: EMC.TO) [Internet], 2014, [cited 2017 February 01], http://www.scandiummining.com/i/pdf/Scandium-White-PaperEMC-Website-June-2014-pdf.

5 K. Binnemans, P. T. Jones, B. Blanpain, T. Van Gerven and Y. Pontikes, *J. Cleaner Prod.*, 2015, **99**, 17–38.

6 Y. Liu and R. Naidu, *Waste Manage.*, 2014, **34**, 2662–2673.

7 B. Onghena and K. Binnemans, *Ind. Eng. Chem. Res.*, 2015, **54**, 1887–1898.

8 M. T. Ochsenkühn-Petropoulou, K. S. Hatzilyberis, L. N. Mendrinos and C. E. Salmas, *Ind. Eng. Chem. Res.*, 2002, **41**, 5794–5801.

9 W. Wang and C. Y. Cheng, *J. Chem. Technol. Biotechnol.*, 2011, **86**, 1237–1246.

10 N. Van Nguyen, A. Iizuka, E. Shibata and T. Nakamura, *Proceedings of the World Congress on Mechanical, Chemical, and Material Engineering*, 2015, p.338.

11 J. P. Faris and J. W. Warton, *Anal. Chem.*, 1962, **34**, 1077–1080.

12 V. Korovin and Y. Shestak, *Hydrometallurgy*, 2009, **95**, 346–349.

13 Z. Zhao, Y. Baba, W. Yoshida, F. Kubota and M. Goto, *J. Chem. Technol. Biotechnol.*, 2016, 2779–2784.

14 J. Jerez, A. C. Isaguirre, C. Bazan, L. D. Martinez and S. Cerutti, *Talanta*, 2014, **124**, 89–94.

15 H. Zhou, D. Li, Y. Tian and Y. Chen, *Rare Met.*, 2008, **27**, 223–227.

16 J. Ma, Z. Wang, Y. Shi and Q. Li, *RSC Adv.*, 2014, **4**, 41597–41604.

17 A. N. Turanov, V. K. Karandashev, N. S. Sukhinina, V. M. Masalov and G. A. Emelchenko, *J. Environ. Chem. Eng.*, 2016, **4**, 3788–3796.

18 K. K. Yadav, D. K. Singh, M. Anitha, L. Varshney and H. Singh, *Sep. Purif. Technol.*, 2013, **118**, 350–358.

19 A. N. Turanov, V. K. Karandashev, A. N. Yarkevich and Z. V. Safronova, *Russ. J. Inorg. Chem.*, 2010, **55**, 1305–1311.

20 S. Shahida, A. Ali and M. H. Khan, *J. Iran. Chem. Soc.*, 2013, **10**, 461–470.

21 L. Zhu, Y. Liu, J. Chen and W. Liu, *J. Appl. Polym. Sci.*, 2011, **120**, 3284–3290.

22 S. Riaño and K. Binnemans, *Green Chem.*, 2015, **17**, 2931–2942.

23 T. Vander Hoogerstraete, S. Wellens, K. Verachtert and K. Binnemans, *Green Chem.*, 2013, **15**, 919–927.

24 S. Wellens, B. Thijs and K. Binnemans, *Green Chem.*, 2012, **14**, 1657–1665.

25 P. Davris, E. Balomenos, D. Panias and I. Paspaliaris, *Hydrometallurgy*, 2016, **164**, 125–135.

26 D. Dupont and K. Binnemans, *Green Chem.*, 2015, **17**, 856–868.

27 R.-S. Juang, *Proc. Natl. Sci. Counc., Repub. China, Part A: Phys. Sci. Eng.*, 1999, **23**, 353–364.

28 L. Zhu, L. Guo, Z. J. Zhang, J. Chen and S. M. Zhang, *Sci. China: Chem.*, 2012, **55**, 1479–1487.

29 C. P. Mehnert, R. A. Cook, N. C. Dispenziere and M. Afeworki, *J. Am. Chem. Soc.*, 2002, **124**, 12932–12933.

30 A. Riisager, *J. Catal.*, 2003, **219**, 452–455.

31 J.-Q. Wang, X.-D. Yue, F. Cai and L.-N. He, *Catal. Commun.*, 2007, **8**, 167–172.

32 C. Van Doorslaer, J. Wahlen, P. Mertens, K. Binnemans and D. De Vos, *Dalton Trans.*, 2010, **39**, 8377–8390.

33 E. Guibal, A. F. Piñol, M. Ruiz, T. Vincent, C. Jouannin and A. M. Sastre, *Sep. Sci. Technol.*, 2010, **45**, 1935–1949.

34 I. L. Odinets, E. V. Sharova, O. I. Artyshin, K. A. Lyssenko, Y. V. Nelyubina, G. V. Myasoedova, N. P. Molochnikova and E. A. Zakharchenro, *Dalton Trans.*, 2010, **39**, 4170–4178.

35 X. Sun, B. Peng, Y. Ji, J. Chen and D. Li, *Sep. Purif. Technol.*, 2008, **63**, 61–68.

36 F. Giacalone and M. Gruttadauria, *ChemCatChem*, 2016, **8**, 664.

37 N. Kabay, J. L. Cortina, A. Trochimczuk and M. Streat, *React. Funct. Polym.*, 2010, **70**, 484–496.

38 M. Cox, *Chem. Eng. J.*, 2001, **84**, 107–113.

39 T. Vincent, A. Parodi and E. Guibal, *Sep. Purif. Technol.*, 2008, **62**, 470–479.

40 A. Ahmad, J. A. Siddique, M. A. Laskar, R. Kumar, S. H. Mohd-Setapar, A. Khatoon and R. A. Shiekh, *J. Environ. Sci.*, 2015, **31**, 104–123.

41 H. Matsunaga, A. A. Ismail, Y. Wakui and T. Yokoyama, *React. Funct. Polym.*, 2001, **49**, 189–195.

42 Q. Cai, W.-Y. Lin, F.-S. Xiao, W.-Q. Pang, X.-H. Chen and B.-S. Zou, *Microporous Mesoporous Mater.*, 1999, **32**, 1–15.

43 P. Nockemann, B. Thijs, K. Van Hecke, L. Van Meervelt and K. Binnemans, *Cryst. Growth Des.*, 2008, **8**, 1353–1363.

44 R. Bogoczek and E. Kociolek-Balawejder, *React. Polym., Ion Exch., Sorbents*, 1987, **7**, 57–62.

45 L. J. Bellamy, *The Infra-red Spectra of Complex Molecules*, Chapman and Hall Ltd., London, 3rd edn, 1975.

46 J. Goworek, A. Kierys, W. Gac, A. Borówka and R. Kusak, *J. Therm. Anal. Calorim.*, 2009, **96**, 375–382.

47 S. Liang, J. Xu and J. Chen, *J. Therm. Sci.*, 2004, **13**, 187–192.

48 D. Depuydt, W. Dehaen and K. Binnemans, *Ind. Eng. Chem. Res.*, 2015, **54**, 8988–8996.

49 J. S. Preston, *Hydrometallurgy*, 1985, **14**, 171–188.

50 T. Vander Hoogerstraete, B. Onghena and K. Binnemans, *Int. J. Mol. Sci.*, 2013, **14**, 21353–21377.

51 A. El Kadib, P. Hesemann, K. Molvinger, J. Brandner, C. Biolley, P. Gaveau, J. J. E. Moreau and D. Brunel, *J. Am. Chem. Soc.*, 2009, **131**, 2882–2892.

52 P. R. Haddad and P. E. Jackson, *Ion Chromatography: Principles and Applications*, Elsevier, Amsterdam, 1st edn, 1990.

53 P. Nockemann, B. Thijs, S. Pittois, J. Thoen, C. Glorieux, K. Van Hecke, L. Van Meervelt, B. Kirchner and K. Binnemans, *J. Phys. Chem. B*, 2006, **110**, 20978–20992.

54 G. W. Bodammer and R. Kunin, *Ind. Eng. Chem.*, 1953, **45**, 2577–2580.

55 R. Hema Krishna and A. V. V. S. Swamy, *Int. J. Eng. Res. Dev.*, 2012, **4**, 29–38.

56 N. Takeno, Atlas of Eh-pH diagrams: Intercomparison of thermodynamic databases, [Internet] 2005 [Cited 2017 February 01], http://www.eosremediation.com/download/ Chemistry/Chemical%20Properties/Eh_pH_Diagrams_pdf.

57 J. Roosen, S. Van Roosendael, C. R. Borra, T. Van Gerven, S. Mullens and K. Binnemans, *Green Chem.*, 2016, **18**, 2005–2013.

58 J. Liu, X. Yang, X. Cheng, Y. Peng and H. Chen, *Anal. Methods*, 2013, **5**, 1811–1817.

59 J. Zhang, B. Zhao and B. Schreiner, *Separation and hydrometallurgy of rare earth elements*, Springer International Publishing AG, Switzerland, 2016.

60 S. Schrodle, W. Wachter, R. Buchner and G. Hefter, *Inorg. Chem.*, 2008, **47**, 8619–8628.

61 B. N. Kumar, S. Radhika, M. L. Kantam and B. R. Reddy, *J. Chem. Technol. Biotechnol.*, 2011, **86**, 562–569.

62 G. Alberti, V. Amendola, M. Pesavento and R. Biesuz, *Coord. Chem. Rev.*, 2012, **256**, 28–45.

63 S. W. Benson, *The Foundations of Chemical Kinetics*, McGraw-Hill, New York, 1st edn, 1960.

64 Y. Ho and G. McKay, *Process Biochem.*, 1999, **34**, 451–465.

65 A. Balouch, M. Kolachi, F. N. Talpur, H. Khan and M. I. Bhanger, *Am. J. Anal. Chem.*, 2013, **04**, 221–228.

66 N. V. Nguyen, A. Iizuka, E. Shibata and T. Nakamura, *Hydrometallurgy*, 2016, **165**, 51–56.

67 D. I. Srnirnov and T. V. Molchanova, *Hydrometallurgy*, 1997, **45**, 249–259.

68 R. Navarro, I. Saucedo, C. Gonzalez and E. Guibal, *Chem. Eng. J.*, 2012, **185–186**, 226–228.

69 A. R. Vaino and K. D. Janda, *J. Comb. Chem.*, 2000, **2**, 579–596.

70 X. Y. Yang, P. Zhang, L. Guo, H. Zhao, Y. Zhang and J. Chen, *Trans. Nonferrous Met. Soc. China*, 2012, **22**, 3126–3130.

71 R. M. Barrer and J. Klinowski, *J. Chem. Soc., Faraday Trans. 1*, 1974, 2080–2091.

72 D. W. Smith, *J. Chem. Educ.*, 1977, **54**, 540–542.

73 B. J. Teppen and D. M. Miller, *Soil Sci. Soc. Am. J.*, 2006, **70**, 31–40.

74 C. R. Borra, B. Blanpain, Y. Pontikes, K. Binnemans and T. Van Gerven, *J. Sustain. Metall.*, 2016, **2**, 28–37.

75 W. Zhang, R. Koivula, E. Wiikinkoski, J. Xu, S. Hietala, J. Lehto and R. Harjula, *ACS Sustainable Chem. Eng.*, 2017, **5**, 3103–3114.

76 W. Zhang, R. Koivula, E. Wiikinkoski, J. Xu, S. Hietala, J. Lehto and R. Harjula, *Proceedings of the Bauxite Residue Valorisation and Best Practices Conference*, [Internet], [cited 2017 July 07], 2015, http://conference2015.redmud.org/wp-content/uploads/2015/10/PS7_Preliminary-investigation-of-rare-earth-separation-by-titanium-phosphate-materials-pdf.